Numerical Analysis of the Relationship between the Photoelectric Effect and Energy of the X-Ray Photons in CT

Rezvan Ravanfar Haghighi [1], Sabyasachi. Chatterjee [2], Pratik Kumar [3], Vani Varadhan Chatterjee [4,*]

1. (a) Medical Imaging Research Center, Radiology Department, (b) Colorectal Research Center.
Namazee Hospital, Shiraz University of Medical Sciences, Shiraz, Iran.
2. BGVS, Chemical Engineering Building (Old), Indian Institute of Science, Bangalore 560 012. India.
3. Medical Physics Unit, Dr B.R. Ambedkar IRCH, All India Institute of Medical Sciences, Ansari Nagar, New Delhi 110 029, India.
4. Department of Instrumentation and Applied Physics, Indian Institute of Science, Bangalore 560012, India.

Received: August 21 2014
Accepted: October 11 2014

Keywords:
X-ray,
DECT,
Photoelectric Effect,
Compton Effect,
Exponents.

ABSTRACT

Purpose: Attenuation of x-rays in any object is a combined effect of scattering and absorption of x-ray photons by the atoms in the material. While the scattering part dependents linearly upon the material's electron density (ρ_e) and is weakly dependent on the energy (E) of the photon, the photoelectric part varies as $[\rho_e Z^x_{eff}/E^y]$ where Z_{eff} is the effective atomic number of the material. We aim to determine the exponents (x,y) which are crucial for many radiological studies.

Methods: In order to obtain exponent *'y'*, we find an equation in which the exponent x does not appear and the dependence on *'y'* appears only linearly. Having thus reduced the problem to that of 'one parameter fit' in *'y'*, we generate the 'data' numerically from the numerical values of physical constants given in the NIST (The National Institute of Standards and Technology, or NIST) tables and determine *'y'* from linear regression. The effect of the source spectrum on the effective value of *'y'*, denoted by 'y_m' is studied for different low Z_{eff} substances in different energy ranges.

Results: It is seen that with x-ray sources operating at 80, 100,120,140 *kVp*, the effective exponent *'y'* progressively decreases, as the x-ray source spectrum is pushed to higher energy side. However, for most practical purposes y=2.99 may be used for a wide variety of low Z_{eff} substances. For practical cases with different source spectra, the effective energy of the source and the effective photoelectric exponent are seen to increase as the thickness of the aluminum filter increases.

Conclusion: It thus follows that for applications such as DECT inversion, the appropriate values of 'y_m' ought to be used that takes into account the appropriate source spectrum.

1. Introduction

Computed Tomography (CT) uses collimated narrow beams of x-ray to measure the attenuation coefficient of each voxel of the scanned material to obtain high quality cross sectional images produced due to attenuation of x-rays in the material through which it passes. It is known that as monochromatic x-rays pass through a medium by a distance l, the intensity of the radiation falls as, $I(l)= I(0)\ exp[-\ \alpha(l)]$, where $\alpha(l) = \int\mu(l',E)dl'$, the integration being over the entire path of the ray with $0 \leq l' \leq l$ and $\mu(l',E)$ is the attenuation coefficient of the material at the point l' on the path of the ray. The method of Computed Tomography (CT) works on the principle that if the integral $\alpha(l) = \int\mu(l',E)dl'$ be known for all possible sections of the material, then it is possible to obtain by the method of Radon Transform, the attenuation coefficient $\mu(x,y,z:E_2)$ at all points (x,y,z) in the substance [1-9] which was successfully demonstrated by Hounsfield [10-12]. The following possibility was immediately recognized: since the attenuation coef-

**** Corresponding Author:***
Vani Varadhan Chatterjee, PhD
Deparment of Instrumentation and Applied Physics, Indian Institute of Science, Bangalore 560003, India.
Tel: 0091-0-80-22932271 / Fax: +91-80-2360 0135
E-mail: vani@iap.iisc.ernet.in

ficient $\mu(x,y,z: E)$ depends upon the values of the electron density (ρ_e) and the effective atomic number (Z_{eff}) of the material at the point (x,y,z), and the energy E of the photon, two independent measurements $\mu(x,y,z: E_1)$, $\mu(x,y,z: E2)$ at two different energies with $E_1 \neq E_2$ can enable us to solve for the two unknowns (ρ_e, Z_{eff}) thus giving information about the chemical composition of the material[13]. These ideas were enriched by several investigators leading to the emergence of the technique of the Dual Energy Computed Tomography (DECT) [14-16]. Suitability of the above method has seen practical demonstration in several areas , from detection of hidden explosives [17] to non-invasive medical diagnostics [18-23].

The central issue in DECT inversion is based on the following factors that decide the x-ray attenuation coefficient of substances. It is known that while the attenuation due to Compton scattering is linearly dependent on the electron density ((ρ_e), the photoelectric cross section, in addition, has a powerful dependence on the effective atomic number (Z_{eff}), and the energy (E) of the photon, being proportional to $(\rho_e Z^x_{eff} / E^y)$. The question of ascertaining the values for x and y, forms the subject of our continuing investigations, as they are key to the question of DECT [23] inversion and in the present paper we further incorporate the effect of the source spectrum, $S(E,V)$ as that is an issue of practical importance. For hydrogen like atoms it can be exactly shown from theory that x=4 and y=3.5 [24,25] while for other substances the values of x and y can be different because of electronic interactions in atoms. In the existing literature, the values of x and y as proposed by different workers in the field, lie in the range, $3.0 \leq x \leq 3.8$ [26-28] and $3.0 \leq y \leq 3.5$. These uncertainties in (x,y) can lead to large errors in calculating the *photoelectric absorption and thus the problem of DECT inversion can be of questionable accuracy. Thus, to formulate effective inversion strategies for finding* (ρ_e, Z_{eff}) *from the DECT data, it is extremely important to ascertain the exact values of the exponents x and y. This, in summary, serves as the motivation for the present paper.* The present paper makes an exhaustive study of the problem by treating in detail, the variation in the value of y with the change in the energy range of study and the effect of this variation on the HU values of substances, when the source spectrum is taken into account. The impact of these variations on DECT inversion to determine (ρ_e, Z^x_{eff}) is pointed out, where we have focused on low Z_{eff} materials as is the case with most biological samples. We have taken the basic 'data' from the physical tables given by the National Institute of Standards and Technology (NIST) [28] and the energy range is chosen so as to suit the problem of DECT imaging and inversion.

2. Materials and Methods

2.1. Attenuation coefficient μ(E)

The basic equation for the attenuation coefficient $\mu(E)$ (for any element or compound) at any monochromatic energy E is given by [with $r_e = 2.82\times10^{-13}$cm, being the classical radius of the electron and $a_0 = 5.29\times10^{-9}$ cm, being the radius of the electron orbit in the ground state of hydrogen]

$$\mu(E) = \mu_{sc}(E) + \mu_{ph}(E) = \mu_{coh}(E) + \mu_{Comp}(E) + \mu_{ph}(E)$$

$$= \alpha_0 f_{coh}(E)\rho_e + \alpha_0 f_{Comp}(E)\rho_e + \beta_0 f_{ph}(E)[\rho_e Z_{eff}^x] \quad (1)$$

where $\alpha_0 = (8\pi/3)r_e^2 = 66.62\times10^{-26} cm^2$ and $\beta_0 = (256\pi/3)(1/137)a_0^2 = 54.7579\times10^{-18} cm^2$ are constants. The quantity $\mu_{sc}(E)$ which gives the attenuation coefficient due to scattering is composed of two parts, due to the coherent Rayleigh scattering and the incoherent Compton scattering both being linearly dependent on ρ_e , as are represented in the first two terms in *Eq.*(1). The coherent elastic part of the scattering makes negligible contribution in the x-ray regime while the incoherent part can be approximated by Klein-Nishina formula, for free electrons, since the binding energy of electrons in the atom is much smaller than the energy of the x-ray photon. We can thus write, as followed in Reference [29],

$$\mu_{sc}(E) = \alpha_0 f_{coh}(E)\rho_e + \alpha_0 f_{Comp}(E)\rho e \approx \alpha_0 f_{KN}(E)\rho_e \quad (2)$$

where $f_{KN}(E)$ is the Klein-Nishina factor [24-26]. The complete formula for $f_{KN}(E)$ is given in Eq.(2) of Reference [29] and its variation with E is shown graphically in Figure 4 of the same paper. The third term in Eq.(1.) denotes the contribution from the photoelectric effect, the functional form for $f_{Ph}(E)$ is given as,

$$f_R(E) = \left(\frac{I_0}{E}\right)^y \quad (3)$$

with I_0 $(= 13.5\ eV)$ denoting the ionization energy the hydrogen ground state and y is an exponent that needs to be specified, which we aim to determine.

Though some of the formulae given in subsequent sections appear in Reference [29], they are reintroduced here, for the sake of completeness and in view of their importance. From the knowledge of the chemical composition of the substance, the quantities, ρ_e and Z^x_{eff} can be calculated. Consider $c(j)$ to give the concentration of the component j in the mixture (number of molecules of j / total number of molecules) and $n(i, j)$ gives the number of atoms of i present in the jth molecule, then

in terms of the density of the system (mass per unit volume) we can write,

$$\tilde{n}_e = \frac{\tilde{n}}{m_p} \frac{\sum_j \sum_i c(j)n(j,i)Z_i}{\sum_j \sum_i c(j)n(j,i)A_i} \quad (4)$$

and

$$Z_{eff}^{x} = \frac{\sum_j c(j) \sum_i n(j,i) Z_i^{x(i)+1}}{\sum_j c(j) \sum_i n(j,i) Z_i} \quad (5)$$

where Z_i is the atomic number and A_i is the atomic weight of the i^{th} atom, $m_p = 1.67 \times 10^{-24}$ *gm* is the mass of the proton, and *x(i)* is the exponent for the photoelectric effect for element '*i*' while Z_{eff} is the effective atomic number, being the weighted average,

$$Z_{eff} = \left[\frac{\sum_j \sum_i c(j)n(j,i)Z_i^{p+1}}{\sum_j \sum_i c(j)n(j,i)Z_i} \right]^{\frac{1}{p}} \quad (6)$$

It is to be noted that the right hand side (r.h.s) of Eqs. (4) and (5) are quantities fixed by the composition of the substance, while the r.h.s. of Eq.(6) has an arbitrariness due to the freedom to choose the value of *p*. It is necessary to make a consistent definition of Z_{eff}, i.e. insist on a uniform convention for the choice of p. For hydrogen-like atoms, it can be shown theoretically that *p=4*. We shall make this choice *p=4*, throughout and the exponent then follows to be, $x = \{log[Z^x_{eff}]/log[Zeff]\}$, where Z^x_{eff} is calculated from the r.h.s. of equation (5), while Z_{eff} is calculated from the r.h.s. of equation (6), both being calculable if the atomic composition i.e. *{c(j), n(j,i)}* be known.

2.2. Mass attenuation Coefficient *[μ(E)/ρ]*

Due to the smallness of coherent scattering, as will be shown in the Results section, we can neglect the first term in Eq(1). By using Eq. (1) and (4) this we get the mass attenuation coefficient to be,

$$\left[\frac{\mu(E)}{\rho}\right] = \sum w(j) \left[\frac{\mu(E)}{\rho}\right]_j \quad (7.a)$$

where

$$\left[\frac{\mu(E)}{\rho}\right]_j = \left(\frac{1}{m_p M(j)}\right) \left[\alpha_0 f_\delta(E) \sum n(j,i) Z_i + \beta_0 f_\beta(E) \sum n(j,i) Z_i^{x(i)+1}\right] \quad (7.b)$$

is the mass attenuation coefficient of the pure compound *'j'*, $M(j) = \sum n(j,i)Ai$ = molecular weight of the *'j'* th molecule and we have substituted $c(j) = [w(j) / M(j)]$ where *w(j)* is he (weight/weight) concentration of the 'j' th compound and $\sum c(j) = \sum w(j) = 1$. For high energies, we can neglect the coherent scattering and approximate it by the Klein-Nishina formula so that we can approximate $f_{sc}(E) \approx f_{KN}(E)$.

2.3. Estimate Of Exponent Y

As can be seen from Eq. (1) and (3), the photoelectric part of the attenuation coefficient depends strongly upon the values of *x* and *y* [29]. Simultaneous determination of both the unknown exponents *(x,y)* from the experimental data may give rise to cross interference between these two unknowns. It is hence advisable to derive an equation, in which one of the parameters (in this case *x*) is eliminated and then we can use the data in this single parameter equation to find the parameter *y*. Once the value of *y* is fixed, the value of *x* can then be calculated subsequently using the calculated value of *y*.

Equation (1) suggests that at any given energy, the contribution from the photoelectric part can be estimated by subtracting out the scattering part from the known total linear attenuation coefficient of the substance [29]. On knowing the values of density and chemical formula for the substance we can calculate,

$$\Delta\chi(E, Z_{eff}) = \left[\frac{\mu(E)}{\rho}\right] - \left[\frac{\mu(E)}{\rho}\right]_{Sc} = \left(\frac{\rho_e}{\rho}\right)\left(\frac{I_0}{E}\right)^y \beta_0 Z_{eff}^x \quad (8)$$

In order to eliminate the characteristic quantities of the substance like ρ_e, ρ and Z_{eff}, we define the ratio (i.e. for the same substances)

$$R(E, E_0, Z_{eff}) = \frac{\Delta\chi(E, Z_{eff})}{\Delta\chi(E_0, Z_{eff})} \quad (9)$$

which clearly gives us, on using (8) and taking the logarithm,

$$log\,[R(E,E_0,Z_{eff})] = -y\,[log(E) - log(E_0)] \quad (10)$$

The quantity $[\mu/\rho]$ is tabulated in the NIST table, while $[\mu(E)/\rho]_{sc} \approx [\mu(E)/\rho]_{KN}$ can be calculated from the first term in Eq. (9) by using the Klein-Nishina formula. A fit of the type given in Eq.(10) enables us to find the value of *y* by starting with the NIST tables to find the values of mass attenuation coefficient.

By substituting the exponent y and thus calculating, $f_{Ph}(E) = (I_0/E)^y$ in Eq. (8), we are able to calculate Z_{eff}^x by Eq. (11) as follows,

$$Z_{eff}^x = \left[\frac{\Delta\chi(E)}{\beta_0 \times f_{Ph}(E)}\right]\left[\frac{\rho}{\rho_e}\right] \quad (11)$$

where $[\rho/\rho_e]$ can be calculated from Eq.(4). We then have, for the exponent x (allowing for energy dependence in its value),

$$x(E) = \frac{\log\left[Z_{eff}^x\right]}{\log\left[Z_{eff}\right]} \quad (12)$$

$[Z^x_{eff}]$ being evaluated from Eq.(5) and Z_{eff} from equation (6).

2.4. Effect of the Source Spectrum

For practical applications, we must note that x-ray sources are not monochromatic. The x-ray flux is spread over a range of photon energies (E), as given by the source spectrum $S(E, V)$. The quantity $S(E,V)$ is the product of (1) the bare source spectrum $S_0(E, V)$ and (2) the filter function $F(E)$. We can calculate S0(E, V) from the Boone Seibert formula and the filter function is given by $F(E) = exp\,[-\mu_{Al}(E)\, l_{Al}]$ where $\mu_{Al}(E)$ is the attenuation coefficient of aluminum for the photon energy E and l_{Al} is the thickness of the aluminum sheet used for filtration.

These mathematical operations given below will show us the effect of the source spectrum $S(E, V)$ on the different effective energies of the system. We can thus define the mean energy to be,

$$E_m = \frac{\int S(E,V)D(E)EdE}{\int S(E,V)D(E)dE} \quad (13)$$

where $D(E)$ is the detector response efficiency.

In all equations, wherever the symbol <…..> appears, it represents the average, as calculated over the source spectrum. In order to understand the effect of the source spectrum on the photoelectric effect and Compton scattering, we define two other energies E_{ph} (Eq. 14) and E_{KN} such that (Eq. 15),

$$< f_{ph}(V) >= \frac{\int f_{ph}(E)S(E,V)D(E)dE}{\int S(E,V)D(E)dE} = f_{ph}(E_{ph}) \quad (14)$$

$$< f_{KN}(V) >= \frac{\int f_{KN}(E)S(E,V)D(E)dE}{\int S(E,V)D(E)dE} = f_{KN}(E_{KN}) \quad (15)$$

Thus E_{ph} and E_{KN} are the monochromatic energies at which the photoelectric and the Klein Nishina parts of the attenuation coefficient are exactly the same as the respective effects averaged over the source spectrum $S(E,V)$.

The effective value of exponent y, namely y_m, is also affected by $S(E, V)$. This can be expressed as,

$$< f_{Ph} >= \left(\frac{I_0}{E_m}\right)^{y_m} \quad (16)$$

so that y_m can be calculated from

$$y_m = \frac{\log\left(< f_{ph}(V) >\right)}{\log\left(I_0/E_m\right)} \quad (17)$$

by using the calculated values of $<f_{ph}(V)>$ and E_m both of which have the effect of $S(E,V)$ ingrained in them.

3. Results

The summary of the results are presented below.

3.1. Part A.

In estimating as to how the joint effect of both coherent and Compton scattering compares with the Klein-Nishina formula that describes the Compton effect for free electrons, we now define the ratio:

$$R_{Sc}(E) = \frac{\left[\left(\frac{\mu(E)}{\rho}\right)_{coheent} + \left(\frac{\mu(E)}{\rho}\right)_{Compton}\right]}{\left(\frac{\mu(E)}{\rho}\right)_{KN}} \quad (18)$$

in which the numerator can be obtained from the NIST tables and the denominator is calculated from the Klein Nishina formula. For cases where $R_{sc}(E) \approx 1$, we make very little error in replacing the total effect of scattering simply by the Klein-Nishina formula while the level of error for any given E can be estimated by $\Delta(E) = 1 - R_{sc}(E)$. The variation of $\Delta(E)$ with E is displayed in Figure 1 for elements such as carbon, nitrogen, oxygen, hydrogen. We find that the error is quite small for $E > 40\,keV$. For lower energies this error is large. However,

filtering of x-ray sources eliminates this low energy part and the contribution of the coherent part thus becomes unimportant, as is discussed below. For this, we refer to Figure 2, which gives the variation of $\delta(E,V)$ for different elements, in the case of V= 80 kVp for the bare Boone Seibert formula (i.e. without filter) for which $\Delta(E)$ is most pronounced.

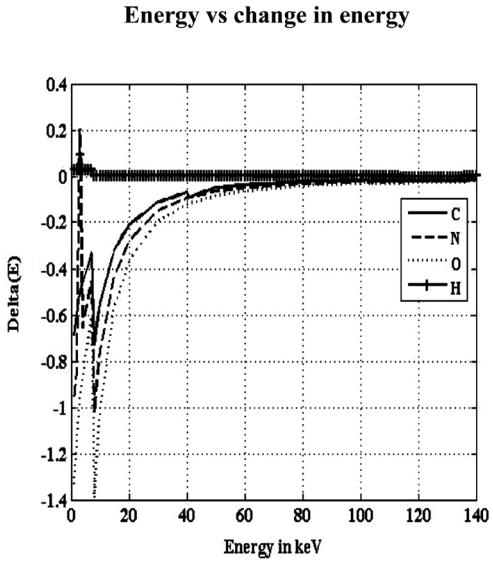

Figure 1. The variation of $\Delta(E)$ versus E for carbon, nitrogen, oxygen and hydrogen for $8<E<80$ keV

We now further define a parameter, [*we assume, D(E) = 1.0,* the detector efficiency being more or less a constant over a wide range or energies, as compared to the variation of the source spectra]

$$\delta(E,V)=\frac{\Delta(E,V)S(E,V)}{\int S(E,V)dE} \qquad (19)$$

which is plotted versus E in Figure 2 for elements H,C,N,O. The quantity $\delta(E,V)$ shows us as to how important the deviation $\Delta(E,V)$ would be when "weighted" by the weightage factor $S(E,V)$, i.e. the source spectrum. We find that $\delta(E,V)$ is very small, everywhere in the whole source spectrum and hence there is very little overall error in using the Klein-Nishina formula to describe the attenuation coefficient due to scattering. It is clear that the average value of $\Delta(E,V)$ is simply $\langle\Delta(E,V)\rangle = \int\delta(E,V)dE$. In Table 1, we display $\langle\Delta(E,V)\rangle$,i.e. the average value of $\Delta(E)$ for $V=80kVp$ with different filters for some low Z_{eff} materials e.g. a fatty acid like acetic acid $(C_2H_4O_2)$, a lipid like cholesterol $(C_{27}H_{46}O)$ and a protein like glycine $(C_2H_5NO_2)$. The largest error appears for $\langle\Delta(E,V)\rangle$ is 0.055, i.e. gives a 5.5% error for oxygen and lower for N,C,H. This error reduces for higher V values, since for higher V the spectrum is pushed to the higher E region. This smallness of $\langle\Delta(E,V)\rangle$ allows us to justify the approximation, $f_{sc}(E) \approx f_{KN}(E)$.

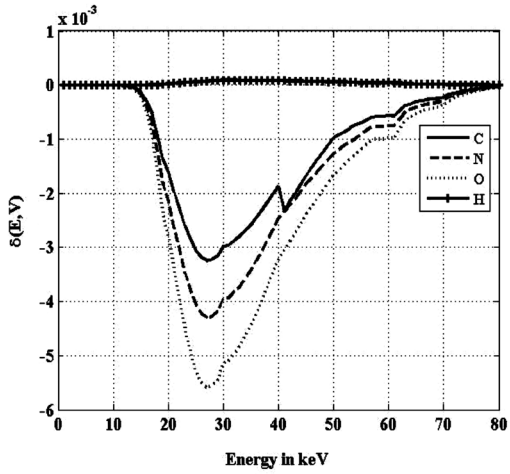

Figure 2. The variation of δ(E,V) with E for H,C,N,O with V=80 kVp , without filter.

Table 1. The presentation of average Δ(E) with l_{Al} = 0.0, 4.0, 8.0, 12.0 mm, for acetic acid ($C_2H_4O_2$), glycine ($C_2H_5NO_2$), cholesterol ($C_{27}H_{46}O$) at 80 kVp excitation voltage.

mmAl	<Δ(E,V)> (Acetic acid)	<Δ(E,V)> (Glycine)	<Δ(E,V)> (Cholesterol ester)
0.0	-0.055	-0.05	-0.03
4.0	-0.04	-0.04	-0.02
8.0	-0.04	-0.036	-0.02
12.0	-0.034	-0.033	-0.01

The results given here are thus in conformity with those given in reference [15] for materials with low effective atomic number.

3.2. Part B.

As discussed under the materials and methods section, Eq. (8) can be used to calculate the mass attenuation

coefficient due to photoelectric effect, by subtracting the mass attenuation coefficient due to scattering from the total mass attenuation coefficient. By this procedure we calculate $\Delta_\chi(E, Z_{eff})$ and $R(E,E_0: Z_{eff})$ from Eq.(8) by using the NIST tables to find the $[\mu(E)/\rho]$ for different substances of low effective atomic number. We have chosen $(6 \leq Z_{eff} \leq 8)$ i.e. substances such as carbon, nitrogen, oxygen, nitric acid, water, acetic acid, sucrose, glycerol *(the suitable range for biological tissues)* and used $[\mu(E)/\rho]_{sc} \approx [\mu(E)/\rho]_{KN}$ as is justified by the numerical results in Part A.

We have used low Z_{eff} materials in this study for all of computations because we are interested in soft tissue characterization, for which these results will be used in future. Attenuation coefficient due to photoelectric effect is strongly dependent on the Z_{eff} of the scanned materials, therefore discrimination between high and low Z_{eff} materials is not so complicated as that between low Z_{eff} ones in the range of x-ray energy used in diagnostic radiology. For this reason we have not considered a case like calcium or iodine, in which photoelectric effect dominates, rendering these substances easily distinguishable from tissues, which are low Z_{eff} materials.

In Figure 3, we plot log[R (E, E_0: Z_{eff}^x)] versus log (E/E_0). We find the unmistakable feature that for any given energy, the ratio R(E,E_0:Z_{eff}^x) and hence *log*[R (E, E_0: Z_{eff}^x)] is insensitive to the nature of the substance at hand (i.e. independent of Z_{eff}). This is seen from the fact that for any given energy the log[R (E, E_0: Zeff)] values are nearly the same for all substances and their data points in Figure 3 nearly overlap. Least square fit is used to calculate the exponent *y*, which can be identified by the log[R (E, E_0: Z_{eff})] vs log (E/E_0) relation, as given in (10) [29-31]. These least square fit curves are shown in Figure 3 and the implications are discussed in later sections.

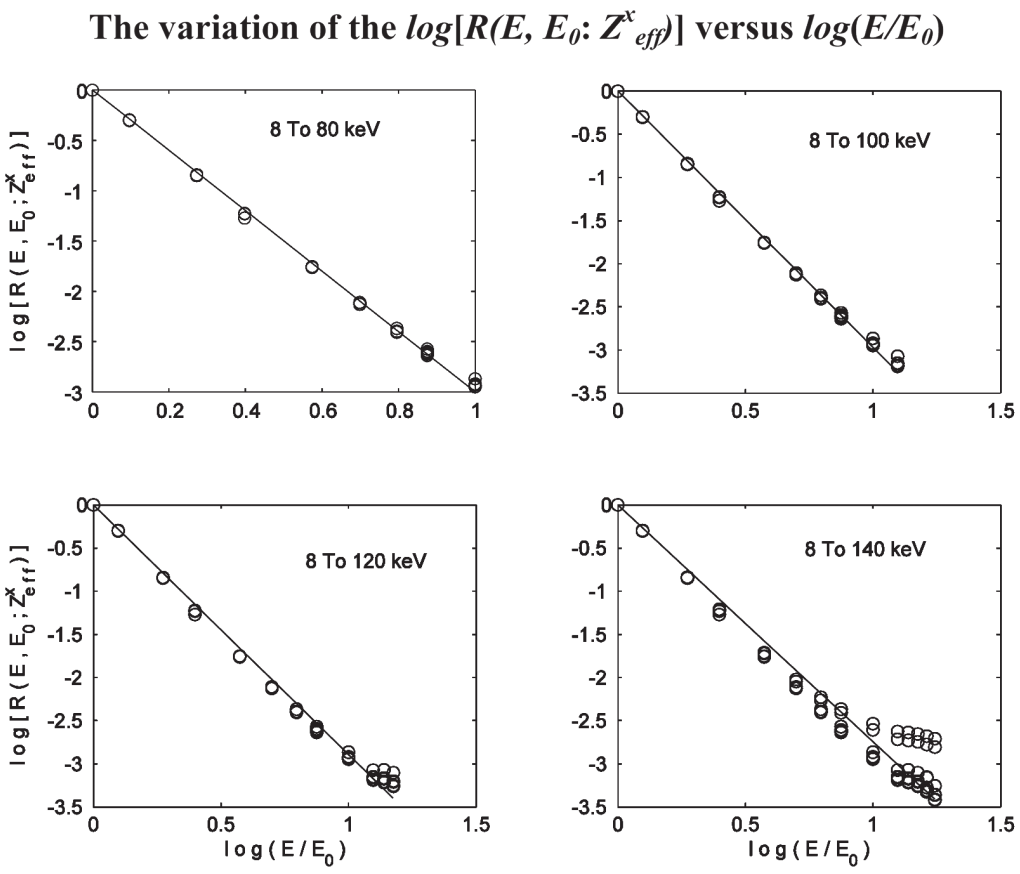

Figure 3. The variation of the log[R(E, E_0: Z^x_{eff})] versus log(E/E_0) for 8 different chemical compounds with low Z_{eff} (carbon, nitrogen, oxygen, nitric acid, water, acetic acid, sucrose and glycerol, all their data being plotted together), for different energies. Most of the data points for different substances (different Z_{eff} values) overlap, showing log[R (E, E_0; Z_{eff})] to be independent of Z_{eff} i.e. of the substance. In this case we have used E_0=8Kev.

As we have explained in the section of the material and method, Eq. (10) is used to calculate the exponent *y*, which is based on the choice of the reference energy E_0. We have calculated the value of the exponent *y* by using E_0=8, 15, 20, 30 keV and the values of y are found to be *y= 2.99, 2.94, 2.93, 2.96* respectively. These are found with 99.99% confidence, there being 72 "data points", with only one variable *(y)* to be fitted. These results are displayed in Table. 2.

Table 2. The calculated values of the exponent y for different choices of E_0.

E0 in keV	Calculated value of y	r	Confidence level in %
8	2.99	0.99	> 99.9
15	2.94	0.99	> 99.9
20	2.93	0.99	> 99.9
30	2.96	0.99	> 99.9

The exponent *y* which is found for different values of E_0(8, 15, 20, 30 keV) is used to calculate the exponent *x* of low Z_{eff} elements and compounds (carbon, nitrogen, oxygen, HNO_3, H_2O, acetic acid, sucrose, glycerol, glycine) by using Eq. (12). The results are shown in Table 3.

Table 3. The exponent x calculated for low Z_{eff} elements and compounds for 8<E<80 keV with y=2.9951, 2.9436, 2.9316, 2.9692, i.e. the exponent values found by taking different values of the reference energy E_0. We have calculated the value of x up to the fourth decimal place and found that on retaining up to the second decimal the error in $(Z_{eff})^x$ does not exceed 1%. Hence we display here the values of x up to the second decimal place.

Substance	Mean *x* as calculated by using different values of *y*			
	y=2.99	*y*=2.94	*y*=2.93	*y*=2.96
C	2.23	2.01	1.96	2.12
N	2.30	2.10	2.05	2.20
O	2.36	2.17	2.13	2.26
HNO_3	2.34	2.15	2.10	2.24
H_2O	2.31	2.12	2.07	2.22
Acetic acid	2.28	2.08	2.04	2.18
Sucrose	2.28	2.08	2.03	2.18
Glycerol	2.27	2.07	2.03	2.17
Glycine	2.28	2.08	2.04	2.18
Average	2.30	2.09	2.05	2.20

The values of *x* and *y* given in Table 3, though close, have differences in the second decimal place. In order to select the most acceptable value, we have performed the following numerical exercise. We selected carbon, nitrogen, oxygen, water, nitric acid, acetic acid, sucrose, glycerol and glycine as test substances and for every set of *(x, y)* values we have calculated [μ(E)/ρ] and found the ratio, $[\mu(E)/\rho]_{cal} / [\mu(E)/\rho]_{NIST}$. We next selected the set for which this ratio is closest to 1. By this exercise we find that the most satisfactory case is given by, *x= 2.30, y= 2.99*. The different values for this ratio in this particular case are given in Table 4.

Table 4. The ratio of $[\mu(E)/\rho]cal / [\mu(E)/\rho]_{NIST}$ calculated with y=2.99 and x=2.3, for different low Zeff materials.

Energy in keV	C	N	O	HNO3	H2O	Ac. Ac	Sucrose	Glycerol	Glycine
8	0.99	1.02	1.03	1.03	1.03	1.02	1.02	1.02	1.02
10	0.96	1.00	1.01	1.01	1.01	1.00	1.00	1.00	1.00
15	0.93	0.96	0.98	0.98	0.98	0.97	0.97	0.97	0.97
20	0.94	0.95	0.96	0.96	0.97	0.96	0.96	0.96	0.96
30	0.97	0.97	0.97	0.97	0.97	0.97	0.97	0.97	0.97
40	0.99	0.99	0.98	0.98	0.99	0.99	0.99	0.99	0.99
50	1.00	1.00	1.00	1.00	1.00	1.00	1.00	1.00	1.00
60	1.01	1.00	1.00	1.00	1.00	1.00	1.00	1.00	1.00
80	1.01	1.01	1.01	1.01	1.01	1.01	1.01	1.01	1.01

We, therefore, use *y=2.99, x=2.30* to calculate *[μ(E)/ρ]* in the subsequent sections of this study, and these values are also to be used as input factors in the DECT inversion algorithm being developed by us.

3.3. Part C.

In this part we take account of the role played by the source spectrum *S(E,V)* in determining the effective energies E_m , E_{KN}, E_{ph} and the exponent y_m . In our computations we have used the Boone-Seibert formula to calculate the "bare" source spectrum S_0(E,V) while the values of $\mu_{Al}(E)$ are taken from the NIST tables to calculate the filter function *F(E)*. In Figure 4, we represent the variation of *S(E,V)* with *E* for a typical case of , l_{Al} *= 8 mm* with *V= 80,100,120,140 keV*. The case with l_{Al}=0 mm is given in Figure 1 of Reference [29] and the difference between the two can be noted.

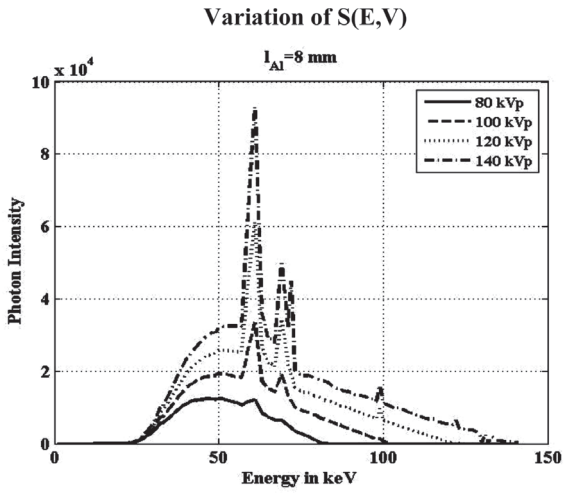

Figure 4. The variation of S(E,V) with E for l_{Al}=8 mm and V= 80, 100, 120, 140 kVp

It is known that filters are effective in eliminating the lower energy part of the spectrum. It is thus necessary to know whether this filtering process will affect the value of the exponent y that we need to use in DECT inversion algorithm, in order to take care of the source spectrum of the filtered x-ray source. The *S(E,V)* for various cases were determined separately and were used as input in Eqs. (13 -15) to calculate the mean values of the photoelectric and Klein-Nishina factors, namely, $\langle f_{ph} \rangle$ and $\langle f_{KN} \rangle$ coefficients as defined in Eqs (14) and (15). The variation of $\langle f_{ph} \rangle$ and $\langle f_{KN} \rangle$ for different excitation voltage V and l_{Al} are shown in Figure 5. The corresponding variations of E_m, E_{KN} and E_{ph} are shown in Figure 6 and those of y_m are given in Figure 7. With increasing *V* and filtering with larger l_{Al} , the source spectrum shifts to the high energy side, $\langle f_{ph} \rangle$ and $\langle f_{KN} \rangle$ both fall monotonically. But $f_{ph}(E) = (I_0/E)^y$ falls rapidly with E as a power law and hence $\langle f_{ph} \rangle$ falls much faster than $\langle f_{KN} \rangle$ while ym is selected to satisfy, $\langle f_{ph} \rangle = (I_0/E_m)^{ym}$.

For some of the practical considerations, it is believed that the effective energy of the source lies between 30%-50% of E_M, where E_M is the maximum photon energy in the source. This assumption has to be qualified in terms of the details of the source spectrum, i.e. by the bare spectrum and the filtration effect and also by the effective energy under consideration. Our detailed calculations show that for E_M and E_{KN}, they lie within 50%-65% of E_M for V=80kVp, between 50% - 60% for V= 100kVp but these come to lie within 42%-55% of E_M for V=120 kVp and within 43%-50% of E_M for V=140kVp, i.e. shifting to the higher energy side as filtration moves the source spectrum the higher energy side. It is seen that due to the rapid decrease of $f_{ph}(E)$ with E , E_{ph} is insensitive to the higher energy photons and E_{ph} lies within 44%-60% of E_M for V= 80kVp, between 40%-51% of E_M for V= 100 kVp, between 33%-46% of E_M for V=120 kVp and between 30% - 50% of E_M for V= 140 kVp. In every case $E_{ph} < E_{KN} < E_{ph}$, as depicted in Figure 6, showing the variation of the respective effective energies in the appropriate ranges within which they lie.

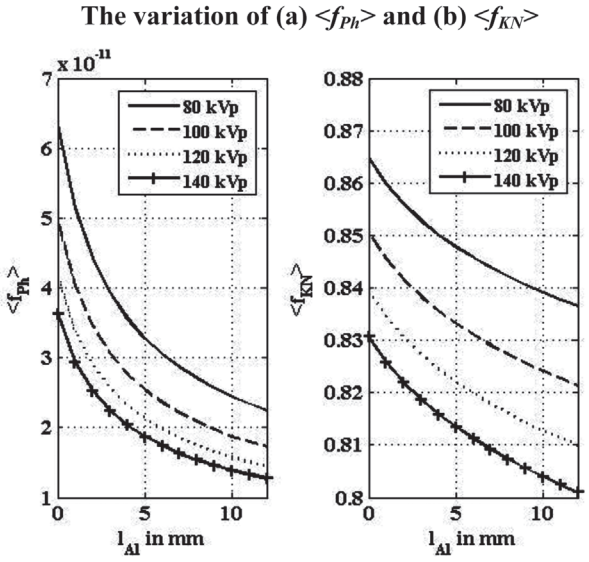

Figure 5. Plots show the variation of **(a)** $\langle f_{Ph} \rangle$ and **(b)** $\langle f_{KN} \rangle$ for different source spectra *S(E,V)* , as generated by placing aluminum filters of thickness lAl in the source, for excitation voltages, V=80,100,120,140 kVp. Some typical source spectra are shown in Figure 2.

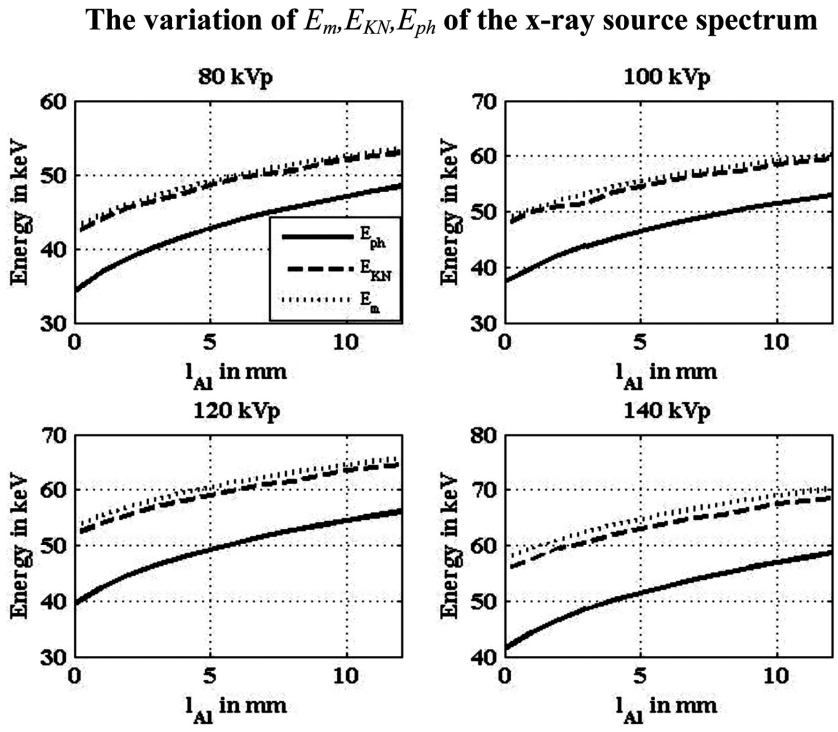

Figure 6. The variation of E_m, E_{KN}, E_{ph} of the x-ray source spectrum for different thicknesses of aluminum filters at 80, 100, 120, 140 kVp excitation voltage.

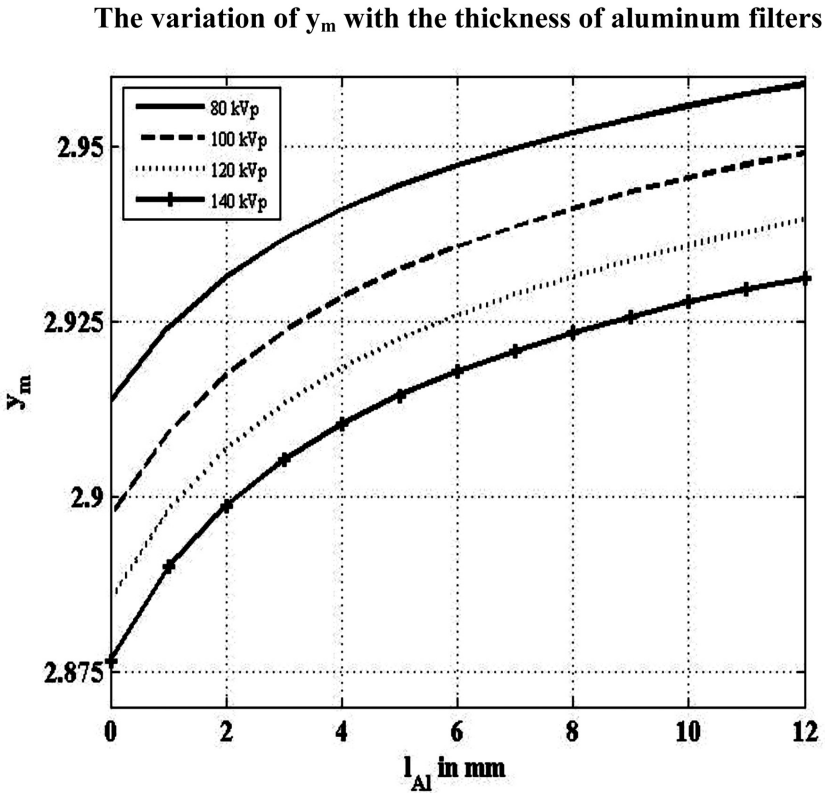

Figure 7. The variation of y_m with the thickness of aluminum filters at V= 80,100,120 and 140 kVp

We end this section on results by demonstrating the practical utility of knowing $\langle f_{KN} \rangle$ and $\langle f_{ph} \rangle$. The attenuation coefficient $\mu(E)$, as given by Eq.(1) is true for any monochromatic energy. The CT machine being polychromatic, it records the average attenuation coefficient over the source spectrum $S(E,V)$ and displays the HU values.

In Table 5 we show the calculated $\langle \mu(100) \rangle$ and $\langle \mu(140 \rangle$ of different low Z_{eff} materials. such as, acetic acid, glycerol, ethanol and a 30% aqueous solution of sucrose and of water. In these calculations we have used,

$$\langle \mu(V) \rangle = \alpha_0 \rho_e \langle f_{KN}(V) \rangle + \beta_0 [\rho_e Z_{eff}^{x}] \langle f_{ph}(V) \rangle \quad (20)$$

with $x=2.30$, $y=2.99$. The results for the corresponding HU(V) values are shown in Table 6. For these calculations we used the above inputs to find $HU(V)=1000\times[\langle \mu(V) \rangle - \langle \mu_w(V) \rangle]/\langle \mu_w(V) \rangle$, for different cases, where the suffix w denotes water.

Table 5. Calculated<(μ(V)> (in cm-1) at 100 and 140 kVp with 0, 4, 8, 12 mm aluminum filter for low Z_{eff} materials such as pure forms of acetic acid (Ac.Ac), glycerol, ethanol, and 30% solution of sucrose in water, water.

mmAl	Pure Ac.Ac		Pure glycerol		Pure Ethanol		30% sucrose		H2O	
	μ100	μ140	μ100	μ140	μ100	μ140	μ100	μ140	μ100	μ140
0	0.29	0.26	0.34	0.30	0.22	0.19	0.33	0.29	0.30	0.27
4	0.24	0.22	0.29	0.26	0.18	0.17	0.27	0.27	0.25	0.22
8	0.22	0.21	0.27	0.25	0.17	0.16	0.25	0.23	0.23	0.21
12	0.21	0.20	0.26	0.24	0.17	0.16	0.24	0.22	0.22	0.20

Table 6. Calculated HU(100) and HU(140) with 0.0, 4, 8, 12 mm aluminum filter for low Z_{eff} materials such as pure forms of acetic acid (Ac.Ac), glycerol, ethanol, and 30% solution of sucrose in water.

mmAl	Pure Ac.Ac		Pure glycerol		Pure Ethanol		30% sucrose	
	HU(100)	HU(140)	HU(100)	HU(140)	HU(100)	HU(140)	HU(100)	HU(140)
0	-45.8	-36.6	129.7	142.3	-283	-268	93	95.7
4	-27.7	-21.7	153	163	-255.5	-244	98	100.5
8	-22	-16	162	170	-244.6	-235	100.5	102
12	-18	-12.6	168	175	-238	-230	102	103.5

The results of the calculated HU (V) for both 100 and 140, with 12 mm aluminum filter, are very close to our experimental finding for the same chemical compounds [31]. These results will also appear in our next communications on DECT inversion which employ the relation (20) and the coefficients $\langle f_{KN}(V) \rangle$, $\langle f_{ph}(V) \rangle$ to determine ρ_e and Z^{x}_{eff}, from the DECT data.

4. Discussion

It is seen that J.F. Williamson et al. [32] observation "the variation of the photoelectric cross section is far more complex than the simple power-law form assumed by the PFM used in this work" is also consistent with our finding that the exponents x, y are not universal constants. We, however, show that for low Z_{eff} materials, for the practical cases of interest, the optimum values $x= 2.30$ and $y= 2.99$ can be used. Since our optimization takes into account the role of the source spectrum, the difficulties associated with the low energy part of energy (see for example Evans et.al [33]) may introduce only marginal errors in the calculation of the photoelectric part of the attenuation coefficient. The photoelectric contribution for low Z_{eff} materials being insignificant the problem remains that "low-Z materials are more sensitive to uncertainties in reconstructed images than high-Z materials" which has thus led us to develop accurate numerical schemes to evaluate the scattering and photoelectric parts of the attenuation coefficient. As pointed out in our earlier paper [29], these uncertainties can lead to gross errors in DECT inversion. The problem is thus treated here in full detail by examining the roles of coherent, incoherent scattering, photoelectric absorption and the effect of the source spectrum. While G. Landry et.al [34] used the ratio [HU(80)/HU(140)] to obtain the quantities (ρ_e, Z_{eff}), accurate DECT inversion must be based on Eq. (20) given in this paper, where the coefficients in the equations take the CT scanners'

source spectrum into account. Since these coefficients are not known and the CT machine simply gives us the HU values, it is necessary to determine them empirically or compute them from the different effective energies that can be calculated, provided the details of the source spectrum are given by the manufacturer. In the work that we will communicate soon, we have experimentally determined these coefficients from which the (ρ_e, Z_{eff}) are accurately determined.

5. Conclusion

The above investigations show that the exponent y is energy dependent and it decreases as the energy range of the x-ray photons increases. For the range of energy between 8 to 80keV, the value of the exponent y is equal to *2.9951*, which is very close to the value of *3.0* that is used in the literature and to the value *y=3.006* which we had found in Ref [29]. The present value is more acceptable, since it is the optimum one, selected after checking the accuracy with different E_0 values. These values *x=2.30* and *y = 2.9951* are the optimum values that can be used for different studies in which the attenuation coefficient comes into play. This is so, since for diagnostic purposes the x-ray sources are operated at voltages less than 140 kVp and the major component of photons lie in the energy range below 80 keV. On increasing the excitation voltage of the x-ray tube and enhancing filtration of the low energy part, the effective energy of the photons increases and the effective photoelectric exponent y also decreases. These properties of the various parameters of the system are contained in the results depicted in Figures 5, 6 and 7 which can be used as inputs for inversion of DECT data, where the aim of the inversion is to determine (ρ_e , Z_{eff}^x) for the purpose of chemical characterization of hidden objects by non-invasive testing.

6. Acknowledgement

Rezvan Ravanfar Haghighi wishes to express her thanks to the Shiraz University of Medical Sciences for the continued support in the course of the present work. She thanks Dr. A.R. Shakibafard and Dr.R. Jalli for their encouragement. Professor J.M.Boone is thanked for providing the program for calculating the source spectrum and Dr. Akondi Vyas is thanked for converting it into MATLAB.

References

[1] J.H.Radon, "Über die Bestimmung von Funktionen durch Ihre Integralwerte laens gewisser Mannigfaltigkeiten" (in German), Berichte über die Vehrhandlungen der Sächcische Wissenschaften (Report of the Proceedings of the Saxony Academy of Sciences), Vol. 69, pp. 262-267, 1917. English translation: R.D.Parks "On the determination of functions from their integral values along certain manifolds", IEEE Transactions on Medical Imaging, Vol.5, pp. 170-176, 1986.

[2] V. Ambartsumian, "On the derivation of the frequency function of space velocities of the stars from the observed radial velocities." Mon. Not. Roy. Astr. Soc. Vol.96, pp,172-179, 1936.

[3] R.N.Bracewell, 'Strip integration in radio astronomy, Australian J. Phys Vol,9, pp.198-217, 1956.

[4] A.M.Cormack, "Representation of a function by its line integrals, with some radiological applications", J.Appl. Phys. Vol. 34, pp., 2722-2727, 1963.

[5] A.M.Cormack, "Representation of a function by its line integrals, with some radiological applications II", J.Appl. Phys. Vol. 35, pp. 2908-2917, 1964.

[6] R.N.Bracewell and A.C.Riddle, "Inversion of fan beam scans in radio astronomy". Astro. phys. J. Vol.150, pp. 427-437, 1967.

[7] G.N.Ramachandran, "Reconstruction of substance from shadow", Proc. Ind. Acad. Sci Section A Vol. 74, pp. 14-24, 1971.

[8] G.N.Ramachandran and A.V.Lakshminarayanan," Three dimensional reconstruction from radiographs and electron micrographs: Application of convolution instead of Fourier transform", Proc Nat. Acad. Sci. USA, Vol. 68, pp. 2236-2240, 1971.

[9] Harrison H Barrett, "The Radon transform and its application" Prog. in Optics, Vol. 21, . E.Wolf Ed, North-Holland, Amsterdam, pp.217-284, 1984.

[10] G.N.Housfield, "Computerized transverse axial scanning (tomography): part1.description of system." British Journal of Radiology, Vol 46, pp.1016-1022, 1973.

[11] A.M.Cormack, "Early two-dimensional reconstruction and recent topics stemming from it", Nobel Lecture, www.nobelprize.org.

[12] G.N.Hounsfield 'Computed medical imaging', Nobel Lecture, www.nobelprize.org

[13] R.A.Rutherford, B.R.Pullan and K.Stierstorfer, "Measurement of effective atomic number and electron density using EMI scanner", Neuroradiology, Vol.11, pp., 15-21, 1976.

[14] B.J.Heismann, J.Leppert and K.Stierstorfer, " Density and atomic number measurements with spectral attenuation method", J.Appl. Phys. Vol. 94, pp. 2073-2079, 2003.

[15] Thorsten R.C.Johnson, Bernhard Krauss etal,"Material differentiation by dual energy CT: initial experience", Eur. Radiol. Vol. 17, pp. 1510-1517, 2007.

[16] M.Bazalova, J.F. Carrier etal, "Dual-energy CT-based material extraction for tissue segmentation in Monte Carlo dose calculation", Phys. Med. Biol. Vol.53, pp. 2439-2456, 2008.

[17] Z.Ying, R.Naidu and C.R.Crawford, "Dual energy computed tomography for explosive detection", Journal of x-ray science and technology Vol.14, pp. 235-256, 2006.

[18] D.E Avin., A.Mcovski and L.E Zatz., "Clinical application of Compton and photo-electric reconstruction in computed tomography: preliminary results", Invest. Radiol. Vol 13, pp. 217-222, 1978.

[19] G.D.Chiro, R.A.Brooks, etal, "Tissue signatures with dual-energy computed tomography", Radiology Vol.131, pp. 521-523, 1979.

[20] M.R.Milner, W.D.McDavid, etal, "Extraction of information from CT scans at different energies", Med. Phys. Vol.6, pp. 70-71, 1979.

[21] S.Oelckers and W.Graeff, "In situ measurement of iron overload in liver tissue by dual-energy methods", Phys. Med. Biol. Vol.41, pp. 1149-1165, 1996.

[22] S.Achenbach, D.Ropers, etal, "Contrast enhanced coronary artery visualization by dual-source computed tomography-initial experience", Eur.J. Radiol. Vol.57, pp.1510-1517, 2007.

[23]. G. Landry, B. Reniers, etal, "Extracting atomic numbers and electron density from a dual source dual energy CT scanner: Experiments and a simulation model", Radiotherapy and Oncology, Volume 100, pp. 375 , 2011.

[24]. B. K. Agarwal, "X-Ray Spectroscopy, An Introduction" Springer-Verlag, Heidelberg, 1991.

[25]. D. F. Jackson and D. J. Hawkes, "X-ray attenuation coefficient of elements and mixtures" Physics Reports Vol. 70 , pp. 169 , 1981.

[26]. H. E. Johns and J. R. Cunningham Physics of radiology, Charles C. Thomas Publisher, Springfield, 1983.

[27]. F. M. Khan, The physics of radiation therapy, Baltimore: Williams and Wilkins, 1994.

[28]. J. H. Hubbell and S. M. Seltzer, "Table of X-ray mass attenuation coefficients from 1keV to 20MeV for elements Z=1 to 92 and 48 additional substances of dosimetric interest"http://physics.nist.gov/PhysRefData/Xcom/html/xcom1.html.

[29]. R. R. Haghighi, S.Chatterjee, etal , "X-ray Attenuation Coefficient of Mixtures: Inputs for Dual-Energy CT", Med Phys, Vol. 38, pp 5270, 2011.

[30]. P. R. Bevington, "Data reduction and error analysis for the physical sciences "McGraw and Hill, New York, 1969.

[31]. Rezvan Ravanfar Haghighi, Ph.D. thesis: "Evaluation of the Coronary Artery Plaque", All India Institute of Medical Sciences, New Delhi, INDIA. 2013.

[32]. Jeffrey F. Williamson, Sicong Li etal, "On two-parameter models of photon cross section: Application to dual-energy CT imaging", Med Phys, Vol. 33, pp.4115, 2006

[33]. Joshua D. Evans, Bruce R. Whiting et. al, "Prospects for in vivo estimation of photon linear attenuation coefficients using post processing dual-energy CT imaging on a commercial scanner: Comparison of analytic and poly-energetic statistical reconstruction algorithm", Med Phys Vol. 40 pp.121914, 2013.

[34]. Guillaume Landry, Joao Seco et.al, "Deriving effective atomic numbers from DECT based on a parameterization of the ratio of high and low linear attenuation coefficients", Phys. Med. Biol. Vol. 58, pp. 6851, 2013.